Optical Simulation and PSF Analysis

Yuanhao Wang

October 15, 2025

1 Experiment

For the evaluation of the results, we consider the Thorlabs LB1761 (a simple BK7 biconvex singlet lens) and perform a simulation using an f/8 aperture placed 2 mm from the second lens surface. We map $[R1, T, R2, D2, OD]$ (mm) as: **R1 = 24.5**, **T = 9**, **R2 = -24.5**, **D2 = 20.5**, **OD = 3.175** (f/8).

We only use **OD = 6.25 mm** for the sampling (N) sweep and off-axis experiments to better illustrate the effects of varying N and off-axis aberrations.

We conducted the following experiments:

- Function test
- Layout & Ray visualization
- Best focus estimation
- Sampling number (N) sweep
- Wavelength (λ) sweep
- Through-focus (D2) sweep
- Aperture sweep (OD)
- Off-axis sweep

Further, we consider a double-Gaussian lens US2532751A, and conducted:

- Wavelength (λ) sweep
- Off-axis sweep

Function Test

Function tests are in `test_geo.py` and `test_ray_tracing.py`, mainly to verify the correctness of the geometric calculations and function implementations.

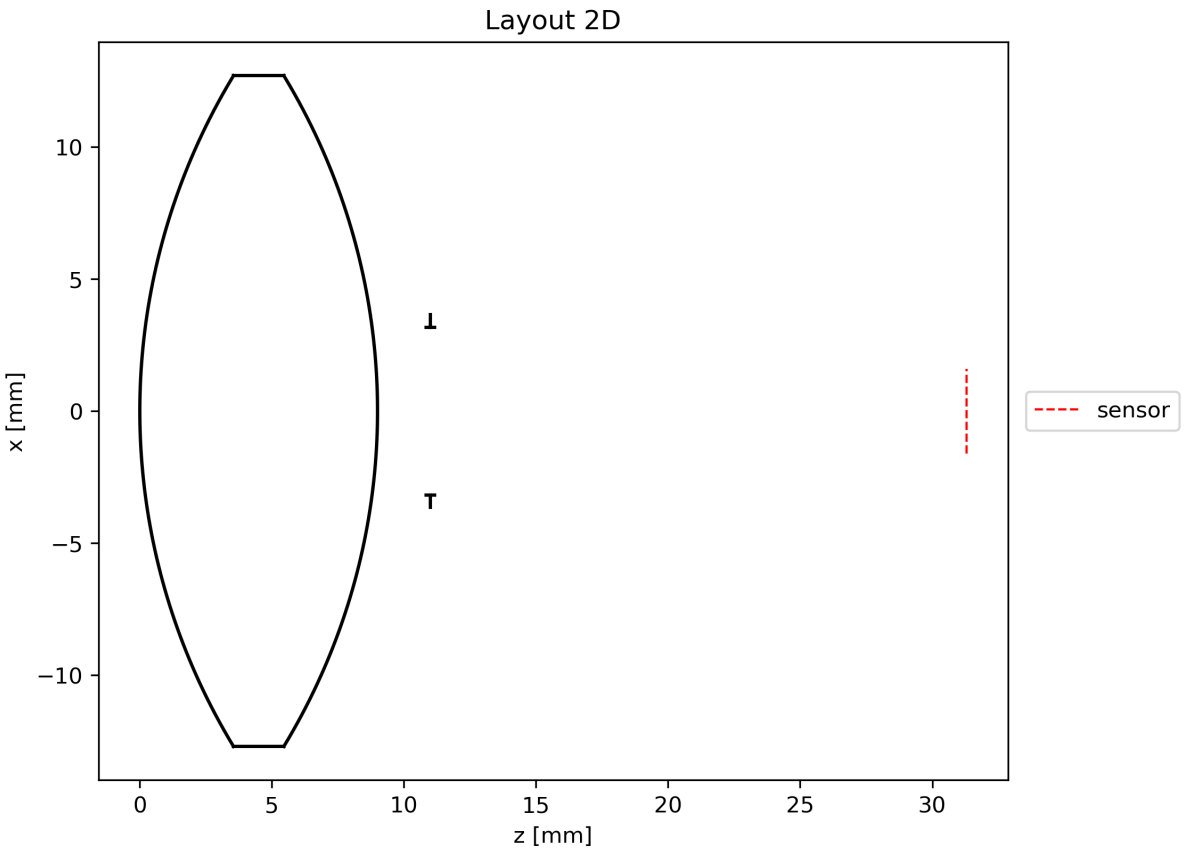

Lens layout.

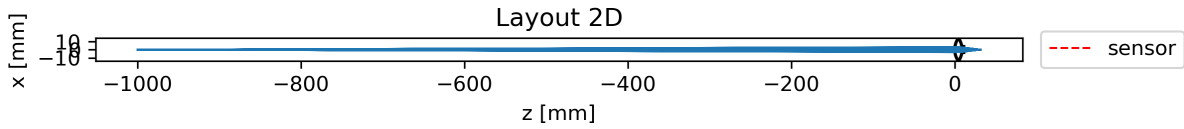

Ray tracing.

PSF Examples

After optimization, placing the sensor (mm) at the following distances *after the aperture* yields the best focus:

Table 1: Best focus distance vs. aperture

Aperture (mm)	**1.6 (f/16)**	**3.175 (f/8)**	**6.35 (f/4)**	**12.7 (f/2)**
Best Focus Distance (mm)	20.55	20.50	20.30	18.70

Observation: The best sensor-to-aperture distance varies slightly with aperture size, shifting from 20.55 mm at f/16 to 18.7 mm at f/2 due to increased spherical aberration at larger apertures.

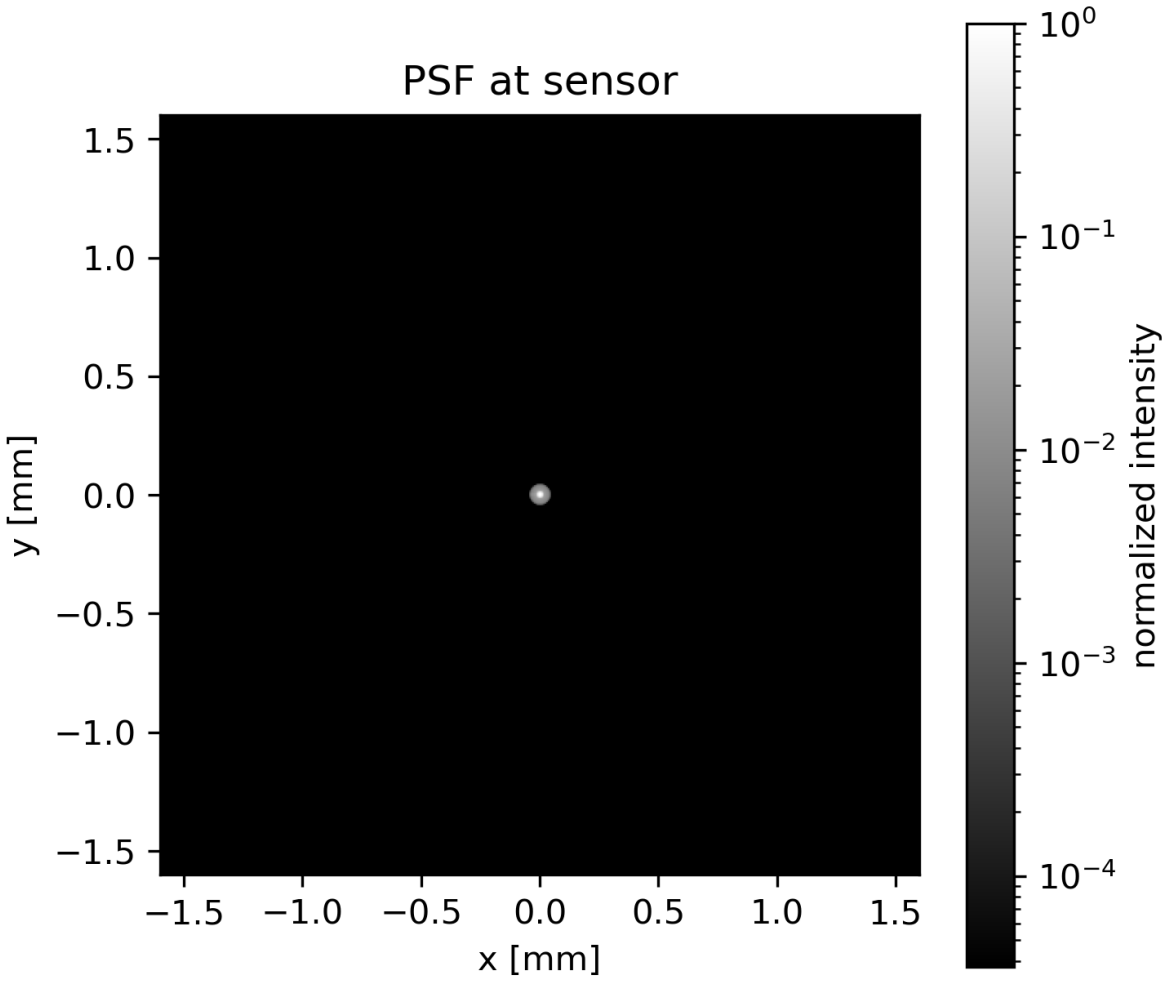

Figure 1: PSF (log scale) at best focus for **3.175 (f/8)** .

N-sweep (sampling)

We swept $N \in \{50, 100, 400, 1600, 3200, 6400\}$ and computed metrics vs. N. To probe focus sensitivity, we also used a larger aperture OD = 6.35 mm D2 = 20.3 mm and repeated the PSF analysis.

Illustrations for $N = \{50, 400, 3200\}$ are shown below (more in the folder):

N = 50	**N = 400**	**N = 3200**
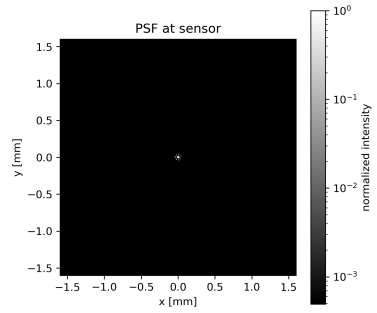	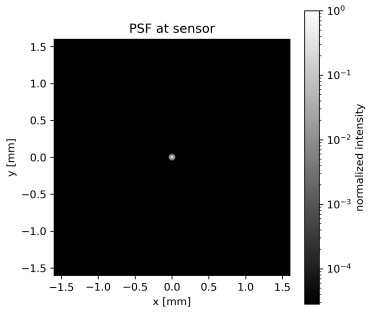	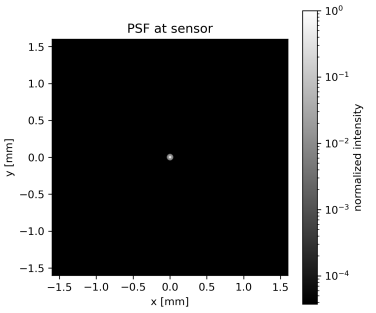

Table 2: PSF snapshots vs. sampling count N.

EE50 and RMS metrics are recorded in `metrics.csv` and plotted in:

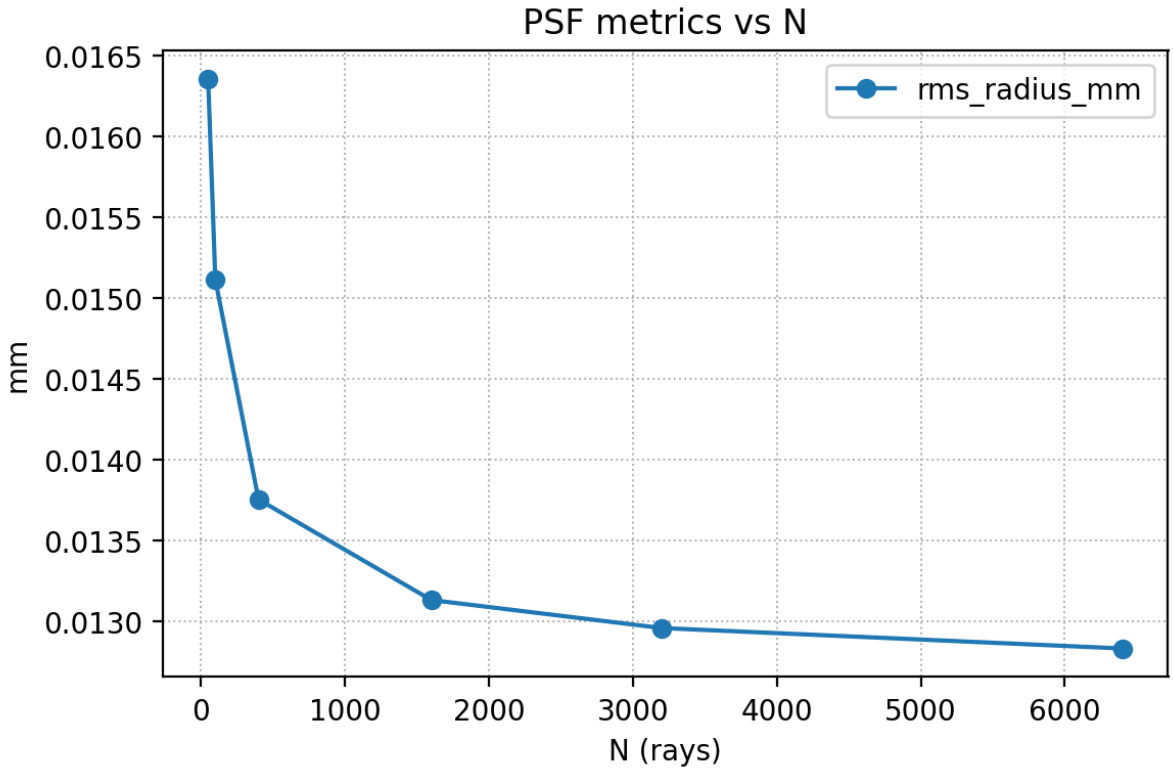

Figure 2: Metrics vs. N.

Observation: The convergence begins around $N \geq 1600$, where RMS values stabilize to $\sim 0.045\,\text{mm}$ and $\sim 0.021\,\text{mm}$, indicating sufficient ray sampling density. We choose $N = 3200$ for the remaining experiments.

Wavelength Sweep

We sweep $\lambda \in \{430, , 670\}$ nm,, with sweep_step $10nm$ (within the visible range):

$\lambda = 430\,\text{nm}$	$\lambda = 520\,\text{nm}$	$\lambda = 610\,\text{nm}$
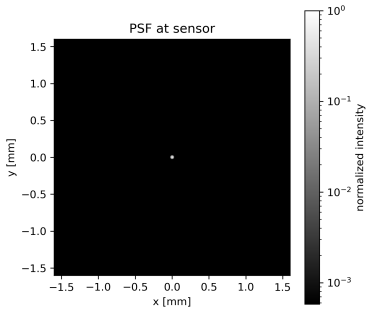	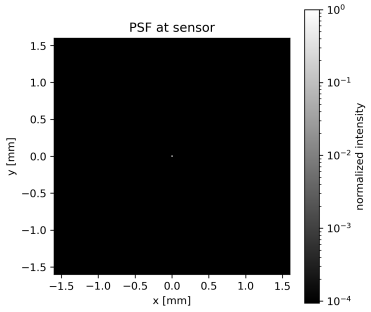	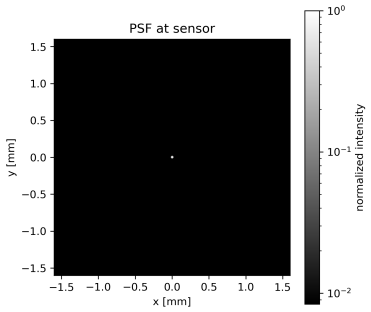

Table 3: PSF vs. wavelength.

Metrics are in `metrics.csv`; plot:

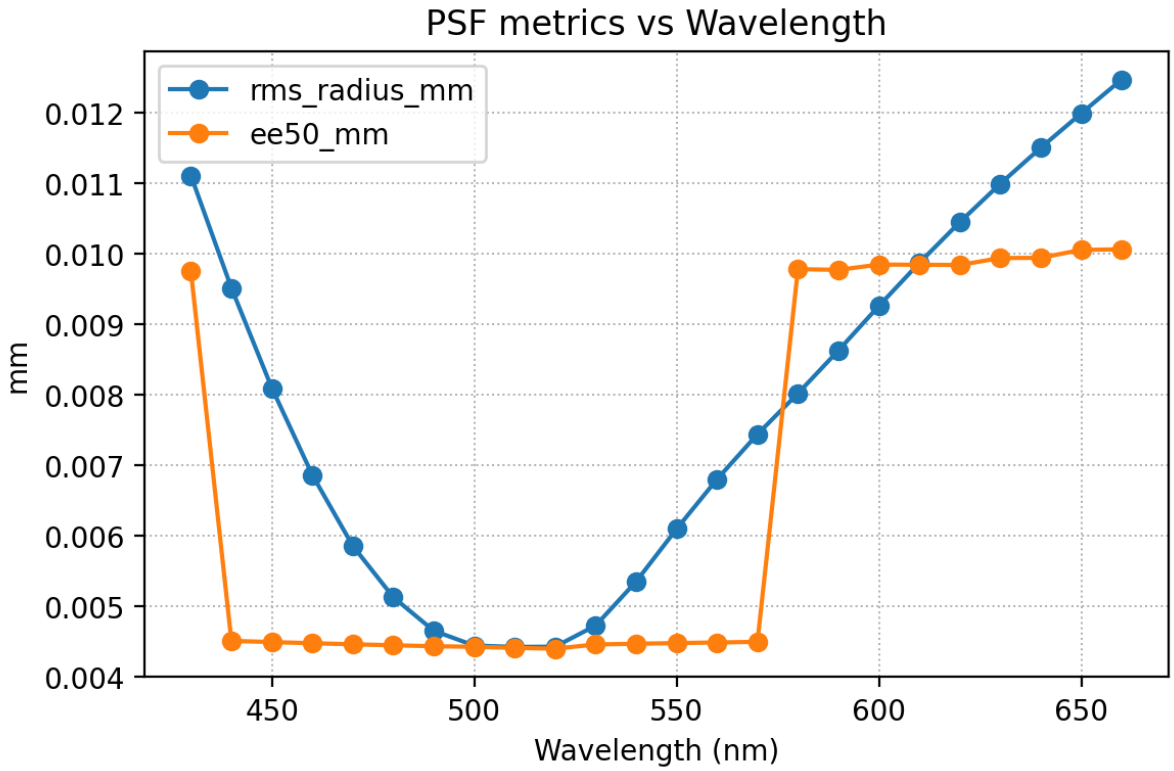

Figure 3: Metrics vs. wavelength.

Observation: With BK7 dispersion enabled, the smallest PSF occurs near $\sim 500\,\text{nm}$ and grows toward both spectral ends (chromatic focus shift).

Through-focus (D2 sweep)

We sweep $D_2 \in [19.5, 21.5]$ mm (sampling 13 steps). The best focus is at $20.5\,\text{mm}$.

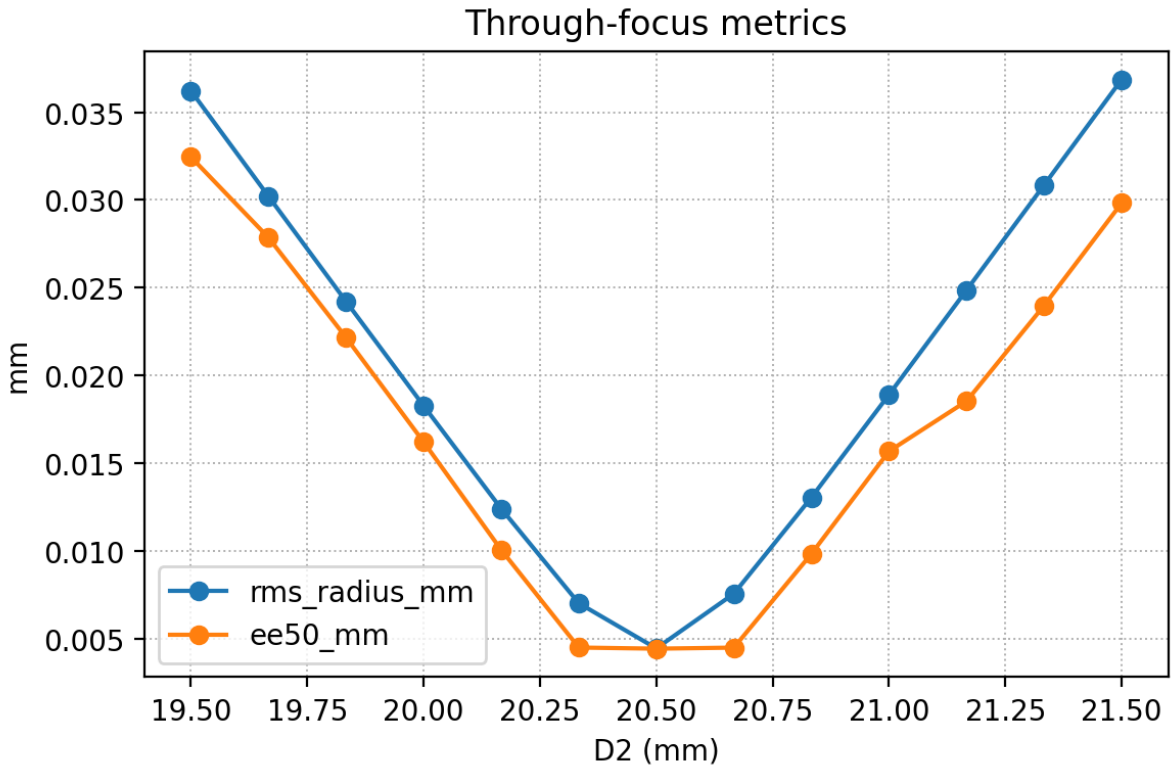

Figure 4: Metrics vs. D_2 (through-focus sweep).

Observation: Moving away from 20.5 mm (e.g., toward 20.33 or 20.66) increases RMS and EE50 smoothly; the curve is slightly asymmetric due to real lens aberrations.

Aperture Sweep (OD)

We sweep OD $\in \{1.5875$ mm $(f/16),\ 3.175$ mm $(f/8),\ 6.35$ mm $(f/4),\ 12.7$ mm $(f/2)\}$.

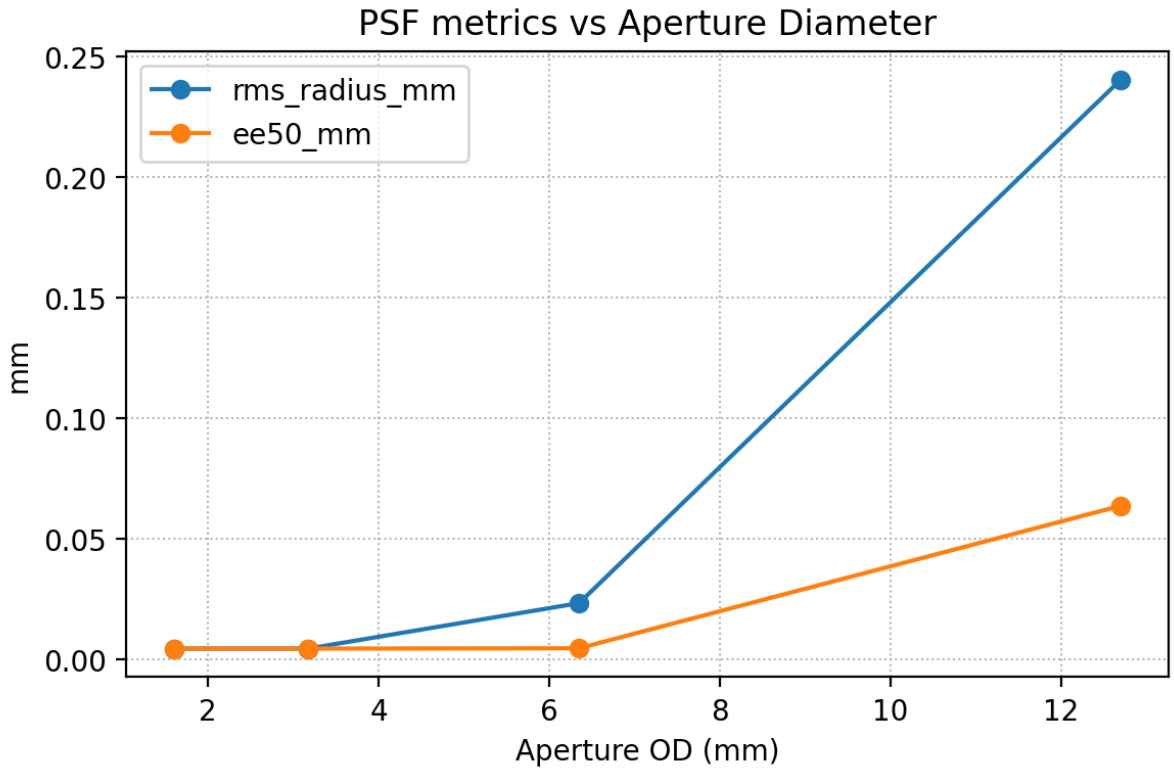

Figure 5: Metrics vs. aperture (OD).

Observation: As aperture increases from ∼1.6 to 12.7mm, the PSF core (EE50) stays nearly constant at small–moderate apertures, while the halo (RMS) grows; at the largest aperture both EE50 and RMS increase noticeably. The sharpest results occur near smaller apertures (∼1.6–3.2 mm).

Off-axis sweep

We consider OD = 6.35 mm $(f/4), R2 = 20.3mm$ for better focus and field offsets $-35, 35$ mm, sampling 36 steps:

Off-axis = −35 mm	Off-axis = 0 mm	Off-axis = 35 mm
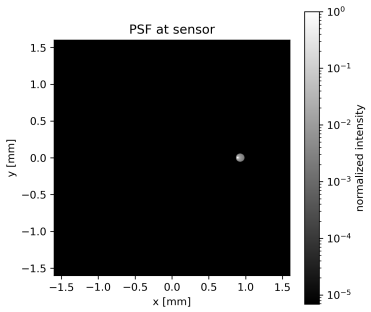	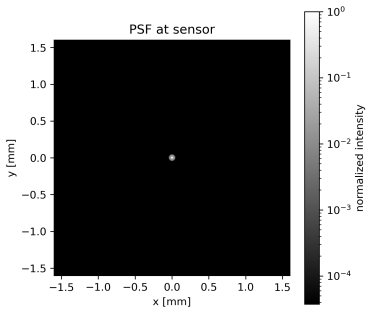	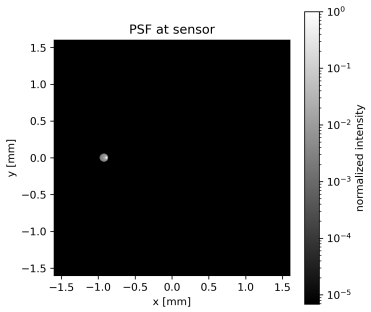

Table 4: PSF vs. field offset (biconvex).

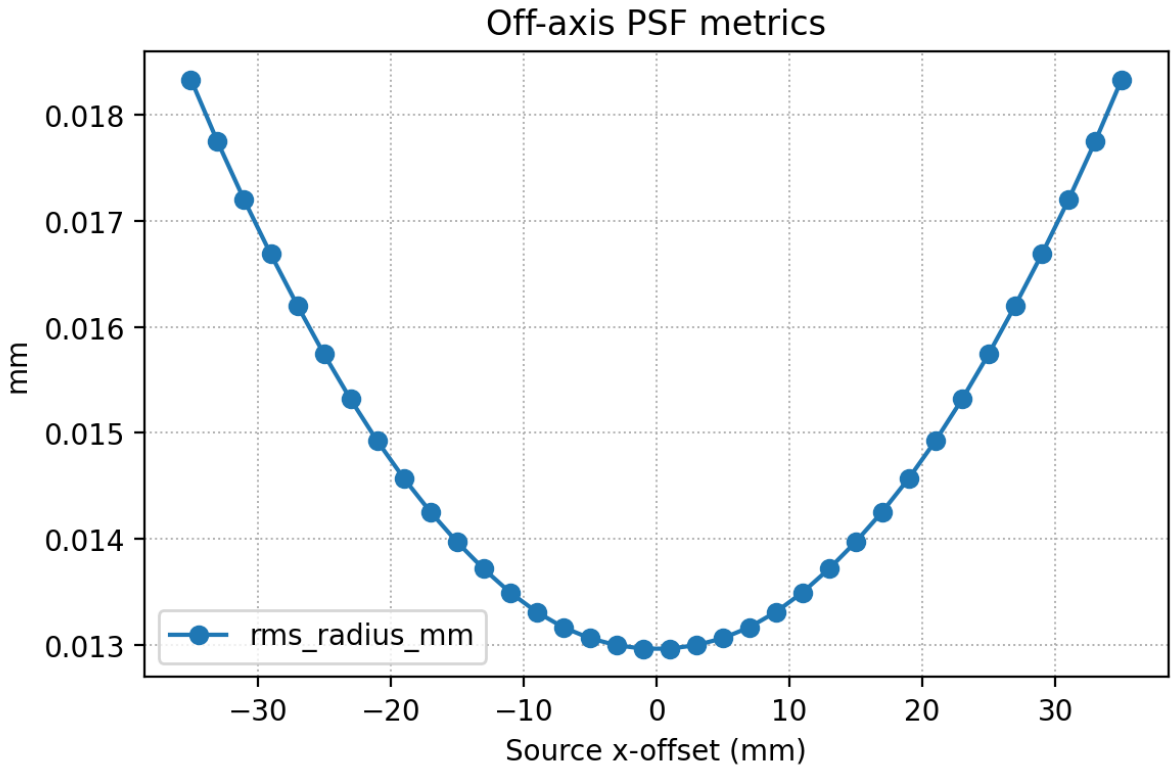

Figure 6: RMS vs. field offset.

Observation: As the source moves off-axis, the PSF centroid shifts roughly linearly with field; core size stays nearly constant for small offsets, with mild coma/asymmetry at larger field.

1.1 Discussion and Qualitative Analysis

Sampling and Aliasing

With small N, the PSF shows speckle-like noise due to non-uniform pupil mapping; as $N \gtrsim 1600$, RMS and EE50 stabilize and the PSF becomes smooth. Mitigations: increase N; average multiple seeds; sample uniformly on the pupil.

Wavelength Dependence (Chromatic Aberration)

With BK7 dispersion, $n(\lambda)$ decreases with λ; effective focal length increases with λ. Thus a fixed sensor plane cannot be perfect for all wavelengths (blue focuses in front; red behind).

Through-Focus Behavior

Sweeping D_2 shows smooth degradation away from best focus (20.5 mm); curves are slightly asymmetric and steeper for larger apertures, matching expectations for residual spherical terms.

Aperture Effect (f-number)

As OD increases from f/16 to f/2:

- EE50 remains nearly constant at small apertures;
- RMS grows at large apertures due to spherical aberration and coma.

Off-Axis Source

Off-axis increases centroid shift and introduces coma at large field; best-focus distance varies mildly across field, indicating slight field curvature. A more complex lens group can suppress these effects (seen in the double gaussian lens experiment).

This indicates a trade-off between brightness and sharpness: smaller apertures (f/8–f/16) yield tighter PSFs and reduced aberrations, while very large apertures (f/2) show blur halos and energy spread.

1.2 Algorithmic Correction of Aberrations

Aberrations (defocus, spherical, coma, astigmatism) broaden PSF and reduce contrast. Modeling as a spatially varying PSF $h(x, y)$, we compare classical vs. learning-based:

Table 5: Classical deconvolution vs. neural approaches

Aspect	**Classical Deconvolution**	**Neural Network Approach**
Principle	Linear inversion (e.g., Wiener, RL) with known PSF	Data-driven mapping from blurred to sharp
Pros	Interpretable; predictable; no training data	Handles complex/chromatic/field-dependent aberrations; flexible
Cons	Sensitive to noise/PSF mismatch; non-stationary PSF is hard	Needs data; potential overfitting
Best use	Mild blur, stationary PSF	Complex scenarios, data-rich pipelines

1.3 Model Refinement and Efficiency

Physical accuracy: include diffraction; model sensor pixel response (e.g., microlens/MTF); consider material tolerances (temperature).
Computation: vectorize intersections; enable GPU acceleration.
Function: extend to scene rendering.

Conclusion

The simulator reproduces key behaviors of the Thorlabs LB1761 singlet and the Double-Gauss configuration. Major outcomes:

- **Functional:** PSF metrics (RMS, EE50); even-grid alignment fix; sampling functions by object distance; `build_lens()`; modular structure; unit tests.
- **Validated optics:** Correct Snell refraction and intersections; PSF metrics converge for $N \geq 1600$; expected trends for wavelength, focus, aperture, and field.

Extra (Double-Gaussian results)

We repeat wavelength and off-axis sweeps on a Double-Gauss (aperture $\approx f/4$).

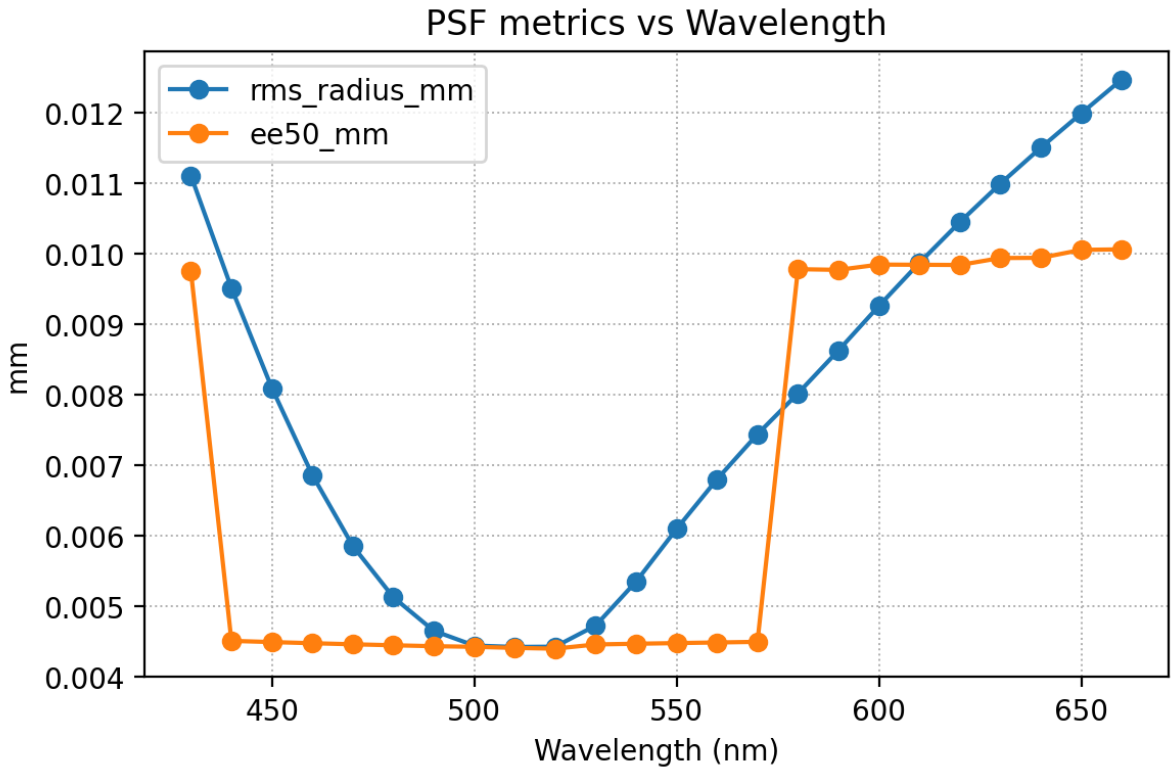

Figure 7: Double-Gauss: metrics vs. wavelength.

Wavelength sweep.

Off-axis = −35 mm	Off-axis = −1 mm	Off-axis = 35 mm
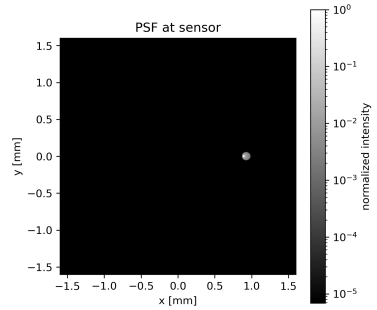	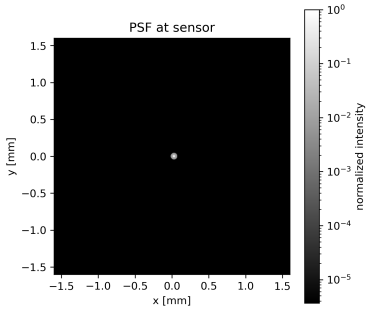	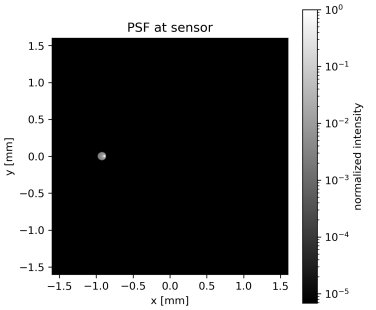

Table 6: PSF vs. field offset (Double-Gauss).

Off-axis sweep. **Observation**: With improved lens design, artifacts such as coma and other aberrations are significantly reduced, yielding better focus consistency across wavelengths—especially evident in the Double-Gauss design.